Membrane Technology
ISSN (online): 1873-4049

Two-dimensional B_5Al_2 as a potential electrode material for lithium-ion batteries

Ziyue Yu, Yu Chen, Yue Yu, Yi Huang*, Zuobin Ning

Key Laboratory of Electronic and Information Engineering, Southwest Minzu University, Chengdu 610041, China

** Corresponding Autho*

Abstract:

In order to meet the requirements of advanced mobile electronic devices and electric vehicles, it is urgent to develop efficient energy storage technique. Lithium-ion (Li-ion) battery is one of most prospected candidates for such a technique. Note that, for the achievement of efficient Li-ion battery, two-dimensional (2D) electrode materials received scientists' attention. In this work, we on the basis of density functional theory (DFT) successfully predicted a new 2D material of B_5Al_2 and evaluated its potential as an electrode material for Li-ion battery. Our results shown that intrinsic B_5Al_2 is metallic and its stability is well confirmed by its ab initio molecular dynamic (AIMD) simulation and phonon spectra calculation. Interestingly, calculated theoretical specific capacity of B_5Al_2 can reach up to 993 mA h/g, and AIMD simulation further confirmed that geometry of B_5Al_2 is well kept at this specific capacity. Meanwhile, we observed that B_5Al_2 always displays a metallic characteristic when it is absorbed by Li ions with various concentrations, which indicates an excellent electrical conductivity during charge and discharge processes. Moreover, we revealed that B_5Al_2 can display a low diffusion energy barrier of 0.05 eV, which is favorable for fast charge and discharge processes. In addition, we also revealed that B_5Al_2 can exhibit a low open-circuit voltage (OCV) with a range from 0.06 to 0.54 V. All of these findings successfully disclose a new 2D metallic material and its superior performances endow it with a promising electrode material for Li-ion battery application.

Keywords: Two-dimensional structure; Electrode material; Lithium-ion battery; Density functional theory

INTRODUCTION

Li-ion battery that benefits from reducing carbon emissions, saving resources, environmental protection and quiet operation has been regarded as an outstanding energy storage technology [1,2]. Currently, Li-ion battery has been widely used in various aspects in modern life, such as smartphones, laptops and new energy vehicles, now [3-7]. In order to achieve efficient Li-ion battery, a key is to found out an advanced electrode material. Note that, traditional electrode materials with ecumenic electrochemical characteristics have cannot meet requirements of efficient Li-ion batteries. For example, graphite is a typical electrode material for Li-ion battery [8,9]. However, its theoretical capacity is only 372 mA h/g, which cannot fully meet a high-performance application that requires extremely high energy density [10,11]. Meanwhile, the capacity decay rate of graphite is relatively fast, which results into a short battery cycle life [12]. Besides, lithium dendrites may appear on graphite electrode, which will puncture the electrode and ultimately result into a worrying safety accident [13]. Thus, it still is urgent to develop new electrode materials with superior electrochemical characteristics [14-16].

Recently, 2D materials have attracted widespread attention due to their unique atomic structures and excellent electronic properties. First of all, larger specific surface area can achieve a large aggregation of lithium ions, which is favorable for the realization of high capacity [17]. Secondly, 2D material can provide a rapid diffusion for lithium ion, which is facilitative for battery's charge and discharge rates [18]. And then, recent studies shown that most 2D materials can possess a good conductivity [19,20]. Finally, some investigations revealed that their lattices can undergo a minimal change during lithium insertion and delithiation, which ensures a stability of material after multiple charge and discharge cycles. At present, renowned 2D materials, such as graphene [21], phosphorene [22], transition metal disulfides [23-25], MXene materials [26-28], have been excellently highlighted as promising electrode materials. Nevertheless, there still some disadvantageous for their practical applications. For example, diffusion energy barrier of graphene is high [29], which might affect its charge and discharge processes. Phosphorene is a semiconductor with a low conductibility, and transition metal disulfides and MXene materials always display low capacities [30]. Therefore, developing high-performance 2D electrode materials for Li-ion batteries is still a challenging task.

Recently, much attention has been paid to 2D III-A group materials [31]. First of all, one of typification is borophene [32]. Various phyletic borophenes, such as honeycomb borophene, β_{12} borophene, δ_6 phase borophene, Pmmn borophene and DMF-exfoliated borophene have been synthesized experimentally [33-35]. In particular, Xu et al. reported possibilities of applications

of Pmmn borophene and DMF-exfoliated borophenes as electrode materials [36]. Subsequently, inspirited by these studies, 2D AlBx materials were proposed and verified as promising host materials for Li-ion batteries. For example, in 2021, Geng et al. successfully deposited 2D AlB_2 nanosheets on a pure aluminum substrate by a mechanical cleavage method [37]. Then the possibility of application of 2D AlB_2 structure as a lithium anode material was explored through first-principles calculations [38]. In 2022, Saeid et al. successfully predicted a 2D AlB_4 structure using a first principles method [39]. Then, Ma et al. explored the possibility of application of 2D AlB_4 as a negative electrode material for Li-ion battery through a first principles method [40]. Recently, 2D AlB_6 structure has been predicted to have high theoretical specific capacity and good stability, which leads it to be an excellent electrode material for Li-ion battery [41]. These findings suggest that 2D III-A group materials can exhibit a significant potential as electrode materials of Li-ion batteries.

In this work, we successfully predicted a new 2D material of B_5Al_2 and confirmed that it is an excellent electrode material for Li-ion battery. We found that intrinsic B_5Al_2 is metallic and AIMD simulation and phonon spectra calculation show that it possesses solid stability. In particular, some excellent electrochemic properties were explored. (a) Calculated theoretical specific capacity of B_5Al_2 can reach up to 993 mA h/g, and AIMD simulation further confirmed that geometry of B_5Al_2 is well kept at this specific capacity. (b) Meanwhile, we observed that B_5Al_2 with various Li adsorption concentrations always displays a metallic characteristic, which indicates a good electrical conductivity during charge and discharge processes. (c) Moreover, we revealed that B_5Al_2 can display a low diffusion energy barrier of 0.05 eV, which is favorable for fast charge and discharge processes. (d) In addition, we also found that B_5Al_2 can exhibit low open-circuit voltages (0.06 ~ 0.54 V). As a result, solid stability and superior electrochemic performances endow it with a promising electrode material for Li-ion battery application.

COMPUTATIONAL METHODS

First principle calculations based on DFT method [42] were performed by Vienna ab initio simulation package (VASP) [43]. The approximate method of generalized gradient approximation (GGA) [44] with the exchange correlation functional of Perdew Burke Ernzerhof (PBE) [45] was used. The cut-off energy of the plane wave [46] was set as 700 eV. For structural optimization calculations, we selected a 11 × 14 × 1 Gamma center k-point grid [47], and for electronic property calculations we used a 14 × 18 × 1 Gamma center k-point grid. The convergence standard of electron was set to be 1.0×10^{-9} eV, and the stress convergence standard acting on each atom in the system was 0.01 eV/Å [48]. In order to eliminate van der Waals force interactions between images, a vacuum layer of approximate 30 Å was established in the z-axis direction. In this work, DFT-D3 method [49] was introduced to handle with the van der Waals interactions. For AIMD simulation [50], the temperature was set to be 300 K. The total simulation time was set to be 20 ps, and the step size was set as 1 fs. Besides, Climbing Image Nudged Elastic Band (CI-NEB) method was used to determine the pathways and corresponding energy barriers of Li diffusion on B_5Al_2 surfaces.

RESULTS AND DISCUSSION

Crystal structure and electronic properties of 2D B_5Al_2 structure

Firstly, we investigated geometric structure and electronic properties of intrinsic B_5Al_2. Figure 1 (a) gives top and side views of optimized B_5Al_2 structure. Clearly, top and bottom surfaces of B_5Al_2 are asymmetric. Its unit cell is a rectangle, and corresponding lattice parameters are a = 3.41 Å and b = 2.90 Å. B_5Al_2 is a six-story structure, which contain two Al layers and four B layers. Calculated bond lengths are listed in Table 1. Electronic properties of B_5Al_2 were explored by investigating its density of states (DOS). As shown in Figure 1 (b), there are many states at the Fermi level, which indicates that B_5Al_2 is intrinsically metallic [51]. Further analysis shown that metallic state is mainly contributed by B 2p state. Besides, we studied its dynamical and thermal stabilities by phonon spectra calculation and AIMD simulation, respectively. Here for phonon spectra calculation, a 4 × 4 supercell combined with 14 × 18 × 1 k-point were used, and for AIMD simulation, a 4 × 4 supercell combined with 11 × 14 × 1 k-point were selected. Corresponding results are listed in Figure 1 (c) and Figure 1 (d). As shown in Figure 1 (c), one can observed that no imaginary frequencies were found in the phonon spectra, which indicates that B_5Al_2 is dynamical stable. As shown in Figure 1 (d), it can be observed that bonds of B_5Al_2 structure at 300 K are nearly not broken, which indicates that B_5Al_2 is thermal stable. As a result, metallic characteristic and solid stability provide reliable guarantees for the application of B_5Al_2 as anode material of Li-ion battery.

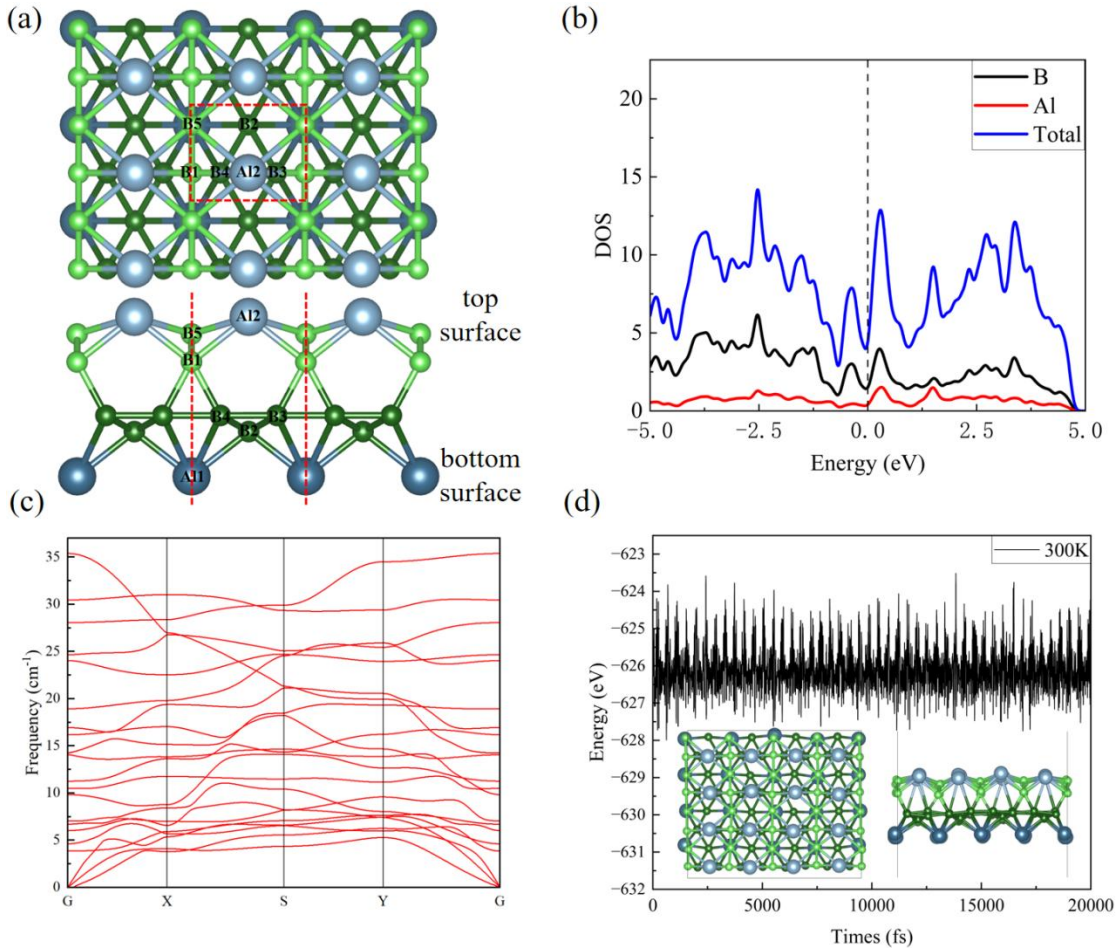

Figure1. (a) Top and side views of optimized 2D B_5Al_2 structure. (b) DOS of 2D B_5Al_2 structure at PBE level. (c) Phonon spectra of 2D B_5Al_2 structure. (d) Energy variation curve of 2D B_5Al_2 structure at 300K. Structural diagram of B_5Al_2 at 20 ps was also listed.

Table 1. Bond lengths, d, of 2D B_5Al_2 structure after structural optimization.

d	$d_{Al2\text{-}B5}$	$d_{Al2\text{-}B1}$	$d_{B5\text{-}B1}$	$d_{B1\text{-}B4}$	$d_{B1\text{-}B3}$	$d_{B4\text{-}B3}$	$d_{B4\text{-}B2}$	$d_{B3\text{-}B2}$	$d_{B4\text{-}Al1}$	$d_{B3\text{-}Al1}$	$d_{B2\text{-}Al1}$	$d_{B3\text{-}Al1}$
(Å)	2.294	2.171	1.669	1.812	1.812	1.692	1.744	1.744	2.476	2.476	2.165	2.165

Adsorption performance of Li atom on 2D B_5Al_2 surfaces

Before studying the electrochemic features of 2D B_5Al_2 structure, we investigated the adsorption performance of single Li atom on B_5Al_2 surface. Here the model was built by putting a Li atom on the surface of a 3 × 3 B_5Al_2 supercell. As shown in Figure 2, eight potential adsorption sites, which include T_A, T_B, T_C, T_D, B_A, B_B, B_C and B_D sties, were considered. Among them, T_A, T_B, T_C and T_D are adsorption sites in which Li locates at top surface of B_5Al_2 structure, and B_A, B_B, B_C, and B_D denote adsorption sites where Li locates at bottom surface of B_5Al_2 structure. In order to determine the most stable Li adsorption site, the adsorption energy of Li atom, E_{ads}, is calculated as follows [52]:

$$E_{ads} = E_{B_5Al_2Li} - E_{B_5Al_2} - E_{Li} \quad (1)$$

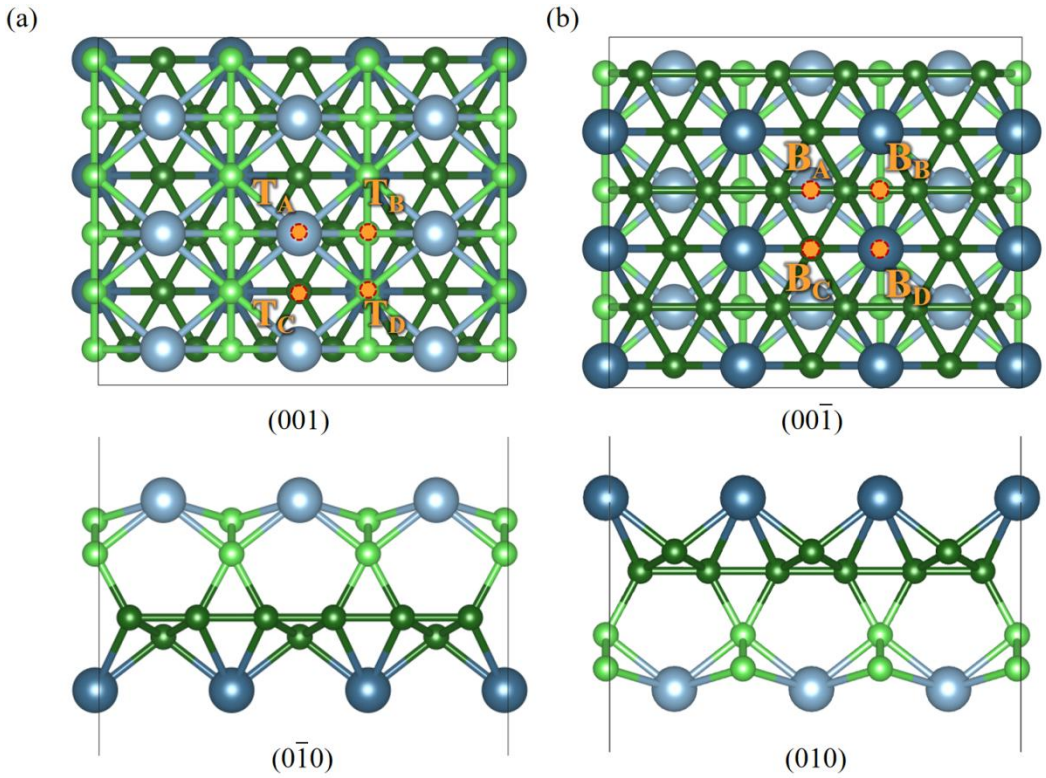

Figure 2. (a) Possible Li adsorption sites on top surface of 2D B_5Al_2 structure. (b) Possible Li adsorption sites on bottom surface of 2D B_5Al_2 structure.

where E_{Li} represents the energy of a single Li atom obtained from Li metal, $E_{B_5Al_2}$ represents the energy of the intrinsic B_5Al_2 structure, and $E_{B_5Al_2Li}$ represents the total energy of whole adsorption system. If the adsorption energy is positive, it means that the adsorption of Li atom on the surface of B_5Al_2 structure is an endothermic process, and if the adsorption energy is negative, it means that the adsorption of Li atom on the surface of B_5Al_2 structure is an exothermic process. As a result, the adsorption energies of T_A and T_C sites are positive and cannot stabilize the adsorption. T_D site with energy of -0.38 eV and B_A site with energy of -0.49 eV are energetically favored sites of Li on top and bottom B_5Al_2 surfaces, respectively. Besides, adsorption energies of Li atom on a 4 × 4 B_5Al_2 supercells were also considered. We found that, for the top surface, Li atom initially positioned on T_A and T_C sites will move to T_B and T_D sites, respectively, after optimizations, and for the bottom surface, Li atom initially positioned on B_A, B_B and B_C sites will move to B_A site. In this case, calculated adsorption energies of Li atom at T_D and B_A sites become -0.40 and -0.49 eV, respectively. Obviously, discrepancies of adsorption energies of Li atoms on 3 × 3 and 4 × 4 B_5Al_2 supercells are small, which confirms the rationality of adsorption model used in this work. Besides, in order to further understand the interaction between Li atom and B_5Al_2 structure, we calculated difference charge densities, as shown in Figure 3. Here yellow and blue regions represent electron enrichment and electron decrease, respectively. Clearly, the charge accumulation occurs at B_5Al_2 structure and the charge loss generates at the Li atom. Thus, considerable electrons of Li atom transfer to that of B_5Al_2 structure when Li atom absorbs on B_5Al_2 surfaces. Obviously, these is a typical ionic interaction between Li atom and B_5Al_2 structure, which explains why Li atom can stably absorb on B_5Al_2 surfaces with low adsorption energies.

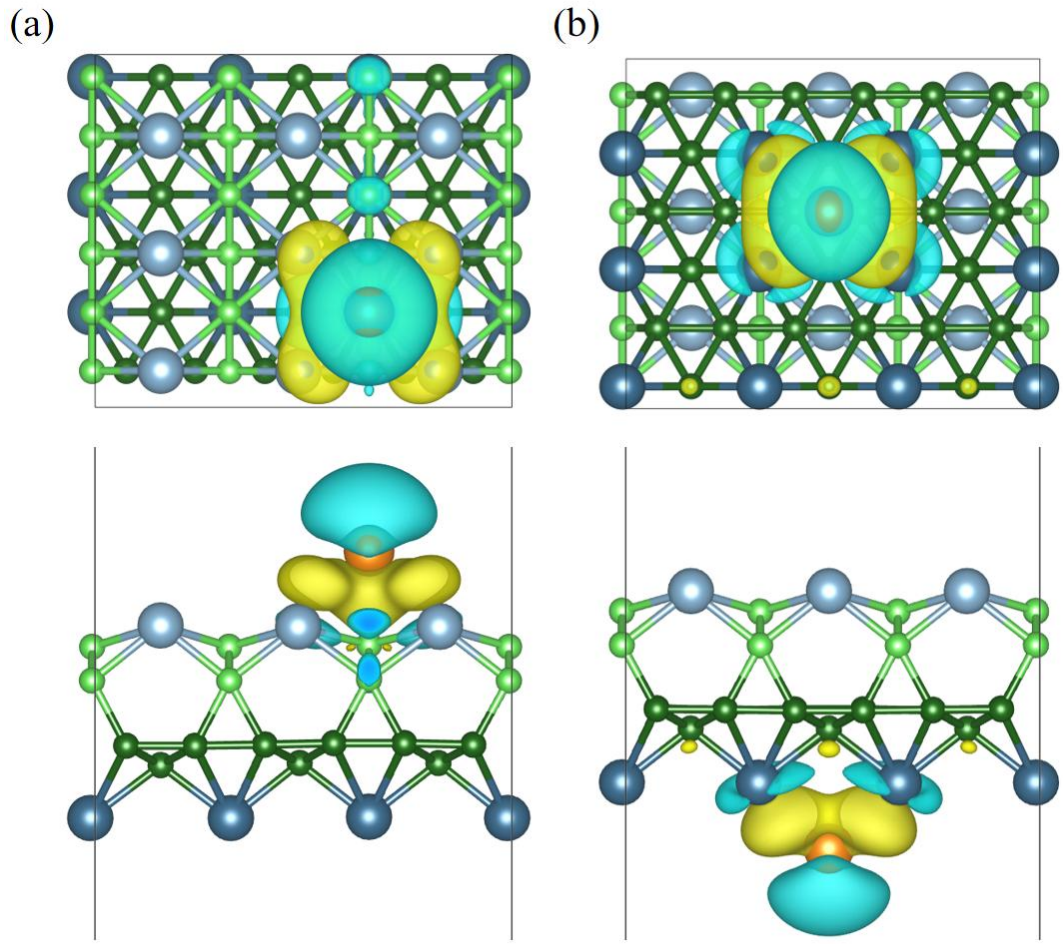

Figure 3. (a) Top and side views of differential charge density of 2D B_5Al_2 structure absorbed with Li atom at the top surface. (b) Top and side views of differential charge density of 2D B_5Al_2 structure absorbed with Li atom at the bottom surface.

Migration ability of Li atom on 2D B_5Al_2 surfaces

Charging and discharging ability, determined by Li diffusion activity, is one of key parameters for evaluating electrochemic performance of an electrode material [53]. To this end, we investigated diffusion activities of Li on top and bottom surfaces of B_5Al_2 structure. Here starting and ending points of the diffusion path were set as most stable adsorption sites [54]. Six representative diffusion paths, namely Path 1, Path 2, Path 3, Path 4, Path 5 and Path 6, were considered, as depicted in Figure 4. Path 1, Path 2, and Path 3 were selected for diffusion of Li atom on B_5Al_2 top surface, and Path 4, Path 5, and Path 6 were chosen for diffusion of Li atom on B_5Al_2 bottom surface. The CI-NEB method was used for all diffusion calculations. Here 5 insertion points were considered and a 3 × 3 B_5Al_2 supercell was applied. Corresponding diffusion barriers are illustrated in Figure 4. Calculated migration barriers of Path 1, Path 2, Path 3, Path 4, Path 5 and Path 6 are 0.05, 0.43, 0.49, 0.23, 0.44 and 0.67 eV, respectively. As we known, the lower the diffusion barrier, the faster the charging and discharging processes. Here, the value of 0.05 eV is extremely low. For example, the value is much lower than that of current commercial graphite electrode material (> 0.32 eV) [55]. Interestingly, it is also lower than those of most reported popular 2D electrode materials, such as WSe_2 (0.24 eV) [56], graphene (0.37 eV) [57], silene (0.25 eV) [58], BC_3 (0.34 eV) [59], GeS (0.24 eV) [60], phosphorene (0.76 eV) [61], Si_2BN (0.32 eV) [62] and Si_3C (0.46 eV) [63]. A small diffusion barrier here means that the Li atom can move quickly on B_5Al_2 surface, which might result into fast charging and discharging processes. As a result, B_5Al_2 served as electrode material can provide a good rate performance for Li-ion battery.

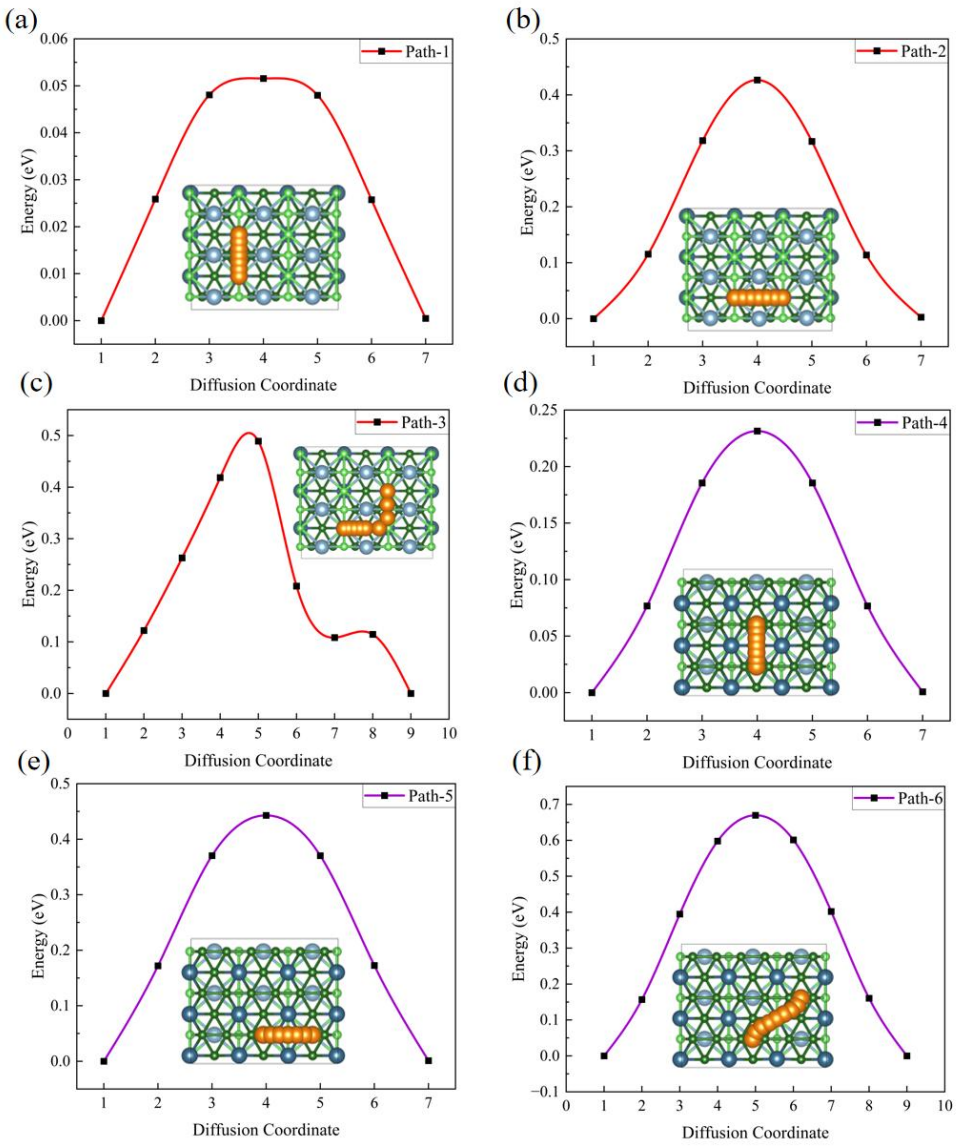

Figure 4. (a) Diffusion path and corresponding diffusion energy barrier of Li on top surface of B_5Al_2 structure along the Path 1. (b) Diffusion path and corresponding diffusion energy barrier of Li on top surface of B_5Al_2 structure along the Path 2. (c) Diffusion path and corresponding diffusion energy barrier of Li on top surface of B_5Al_2 structure along the Path 3. (d) Diffusion path and corresponding diffusion energy barrier of Li on bottom surface of B_5Al_2 structure along the Path 4. (e) Diffusion path and corresponding diffusion energy barrier of Li on bottom surface of B_5Al_2 structure along the Path 5. (f) Diffusion path and corresponding diffusion energy barrier of Li on bottom surface of B_5Al_2 structure along the Path 6.

Theoretical specific capacity of 2D B_5Al_2 structure

Theoretical specific capacity that directly decide the electrochemic performance of Li-ion battery is another critical factor [64]. To this end, we studied the theoretical capacity of B_5Al_2 structure. Here the theoretical capacity was calculated using the following formula [65]:

$$C = (zxF)/M \quad (2)$$

where, z is the valence number (z = 1 for Li), x represents the maximum number of lithium atoms that can be adsorbed by the system, F is the Faraday constant (F = 26801 mA h/g), and M represents the relative molecular weight of host material. First, we considered adsorption performance of 2 Li-layers (8 Li atoms) on B_5Al_2 structure, namely one Li-layer absorbed on top surface of B_5Al_2 structure and the other Li-layer absorbed on bottom surface of B_5Al_2 structure. Figure 5 (a) gives the most stable configuration, in which all Li atoms on B_5Al_2 top surface locate at T_D site and all Li atoms on B_5Al_2 bottom surface

locate at BA site. Corresponding molecular formula can be represented as $B_{20}Al_8Li_8$. According to the equation (2), theoretical capacity of $B_{20}Al_8Li_8$ configuration can be determined as 496 mA h/g. This value is lower than those of Zr_2B_2 (526 mA h/g) [66] and Nb_2C (542 mA h/g) [67], but higher than those of VS_2 (466 mA h/g) [68], Ti_3C_2 (448 mA h/g) [69], Ti_2N (487 mA h/g) [70] and $Ti_3C_2S_2$ (311 mA h/g) [71], with same 2 Li-layers adsorptions. Recent studies shown that it is possible for adsorptions of multiple Li-layers on 2D electrode materials [72,73]. Thus, we also estimated probabilities of adsorptions of multiple Li-layers on B_5Al_2 structure by calculating corresponding average adsorption energies. Here we mainly considered probability of adsorption of additional 2 Li-layers on $B_{20}Al_8Li_8$ structure. In this case, corresponding molecular formula can be represented as $B_{20}Al_8Li_{16}$. The average adsorption energy, Eave, of $B_{20}Al_8Li_{16}$ structure is denoted as:

$$E_{ave} = (E_{B_{20}Al_8Li_{16}} - E_{B_{20}Al_8Li_8} - 8E_{Li})/8 \quad (3)$$

where $E_{B_{20}Al_8Li_{16}}$ and $E_{B_{20}Al_8Li_8}$ are energies of $B_{20}Al_8Li_8$ and $B_{20}Al_8Li_{16}$ structures, respectively. According to the equation (3), calculated values for 4 Li-layers absorbed B_5Al_2 structures is about -0.06 eV. Corresponding configuration is listed in Figure 5 (b).

Negative value indicates that it is possible for the adsorption of 4 Li-layers on B_5Al_2 structure [74]. In this case, theoretical capacity is found to be about 993 mA h/g. Obviously, this value is much larger than the value of 496 mA h/g found on the basis of 2 Li-layers adsorption. Next, we also used AIMD simulations to further investigate stabilities of $B_{20}Al_8Li_8$ and $B_{20}Al_8Li_{16}$ systems. Figure 5 (c) and (d) show energy variation curves of $B_{20}Al_8Li_8$ and $B_{20}Al_8Li_{16}$ systems at 300 K, respectively. It can be seen that variations of energies for both cases are relatively small that they fall in the small ranges. Furthermore, as shown in insets, geometrical structures of both $B_{20}Al_8Li_8$ and $B_{20}Al_8Li_{16}$ systems at 10 ps still remain their initial structural characteristics that in both structures B_5Al_2 doesn't exhibit a structural reconstruction and all Li atoms still stoutly absorb on B_5Al_2 surfaces. Thus, it is expected to exhibit high theoretical capacities on the basis of B_5Al_2 electrode material at room temperature.

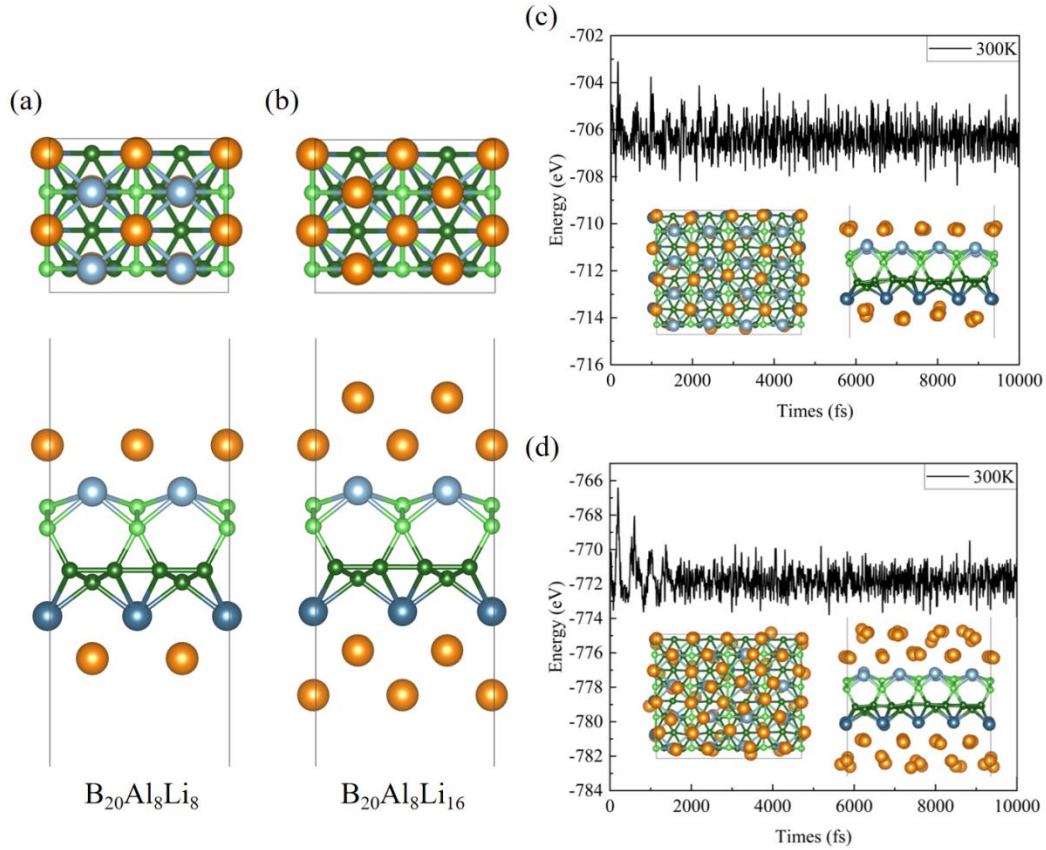

Figure 5. (a) Top and side views of optimized $B_{20}Al_8Li_8$ structure. (b) Top and side views of optimized $B_{20}Al_8Li_{16}$ structure. (c) Energy variation curves of $B_{20}Al_8Li_8$ structure for 10 ps at 300 K. Structural diagram of $B_{20}Al_8Li_8$ at 10 ps was also listed. (d) Energy variation curves of $B_{20}Al_8Li_{16}$ structure for 10 ps at 300 K. Structural diagram of $B_{20}Al_8Li_{16}$ at 10 ps was also listed.

Open circuit voltage and conductivity of 2D B_5Al_2 structure

The open circuit voltage (OCV) is also a key indicator to determine whether Li-ion battery can be efficiently applied. In order to obtain a high operating voltage, the OCV of the electrode material should be low [75]. Here OCV equation is defined as [76]:

$$OCV = E_{Li_{x1}B_5Al_2} - E_{Li_{x2}B_5Al_2} + (x_2 - x_1)E_{L_i} / (x_2 - x_1)e \quad (4)$$

where $E_{Li_{x1}B_5Al_2}$ and $E_{Li_{x2}B_5Al_2}$ are the total energies of $Li_{x1}B_5Al_2$ and $Li_{x2}B_5Al_2$ systems, respectively. Calculated results are shown in Figure 6. One can see that minimal and maximal values of OCV are 0.06 and 0.54 V, respectively. Note that OCV variation here basically falls in a potential range required for the electrode material (0.10 ~ 1.00 V) [77]. Calculated average value of OCV is about 0.30 V, which is also comparable with those of recently reported 2D electrode materials, such as VS_2 (0.93 V) [68], Ti_2N (0.53 V) [70], $Ti_3C_2S_2$ (0.89 V) [71], Mo_2C (0.68 V) [78], Mo_2B_2 (0.93 V) [79]. Thus, it is expectable to obtain high energy output on the basis of B_5Al_2 electrode due to the low OCV value.

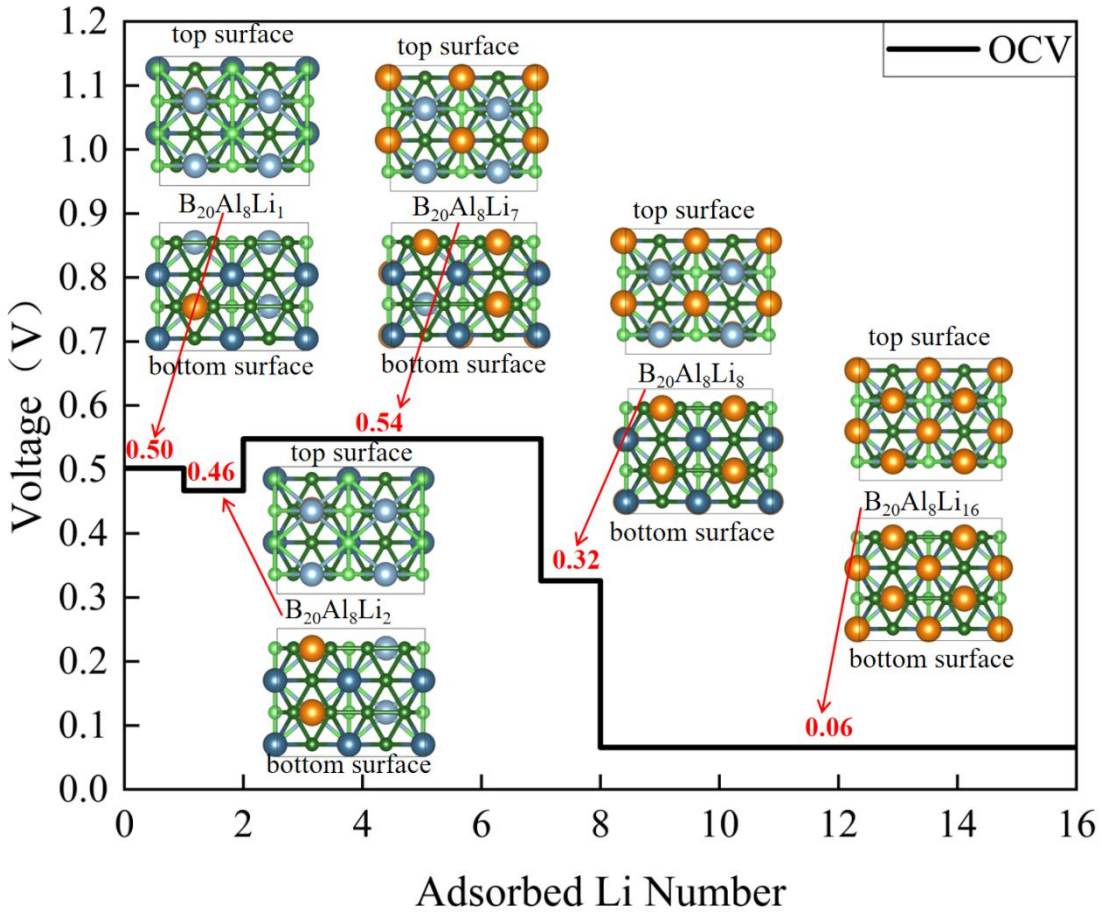

Figure 6. Change trend of OCV with Li adsorption content on B_5Al_2.

Finally, we also investigate conductivity of 2D B_5Al_2 structures under various Li adsorptions by calculating corresponding DOS. We studied total density of states (TDOS) and partial density of states (PDOS) for five adsorption systems, namely $B_{20}Al_8Li_1$, $B_{20}Al_8Li_2$, $B_{20}Al_8Li_7$, $B_{20}Al_8Li_8$, and $B_{20}Al_8Li_{16}$, as shown in Figure 7. One can see that, for all structures, a large number of electron states occur near the Fermi level. Clearly, B atom displays a large contribution, and Al and Li atoms exhibit relatively small contributions. Thus, B_5Al_2 structures under various Li adsorptions still can represent a metallic characteristic, which well meets the requirement of an ideal electrode material.

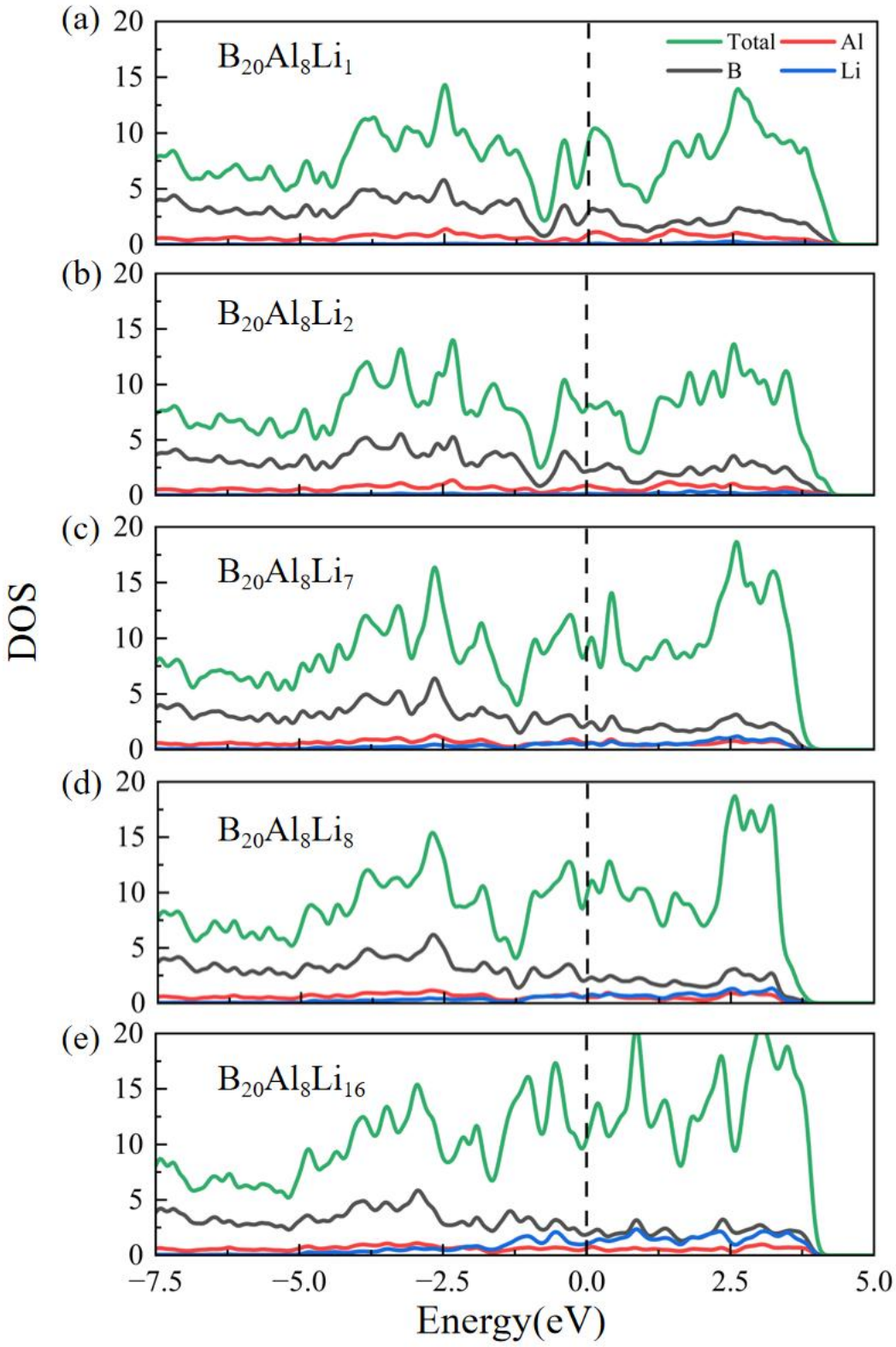

Figure 7. (a) - (e) DOS of $B_{20}Al_8Li_1$, $B_{20}Al_8Li_2$, $B_{20}Al_8Li_7$, $B_{20}Al_8Li_8$ and $B_{20}Al_8Li_{16}$, respectively. The Fermi level is denoted by dashed line.

CONCLUSION

In our study, we, on the basis of DFT method, successfully predicted a new 2D III-A group material and confirmed that it is an ideal 2D electrode material for Li-ion battery. We found that intrinsic B_5Al_2 is metallic and it possesses a good stability.

Interestingly we found that maximal theoretical specific capacity of B_5Al_2 can reach up to 993 mA h/g. AIMD simulation further confirmed that geometry of B_5Al_2 can well be maintained at this specific capacity. B_5Al_2 structures with various Li adsorption concentrations can always display a metallic characteristic, which indicates a good electrical conductivity during charge and discharge processes. An extremely low diffusion energy barrier of 0.05 eV was found when B_5Al_2 was served as a platform for Li diffusion. In addition, we also found that B_5Al_2 can exhibit low open-circuit voltages (0.06 ~ 0.54 V). All of these findings successfully disclose a new metallic 2D structure, which is a highly promising candidate for an electrode material in Li-ion batteries.

CREDIT AUTHORSHIP CONTRIBUTION STATEMENT

Ziyue Yu: Methodology, Data curation, Formal analysis, Writing-original draft. Yu Chen: Software, Preparation, Visualization, Yue Yu: Investigation, Yi Huang: Conceptualization, Resources, Review & editing. Zuobin Ning: Supervision.

DECLARATION OF COMPETING INTEREST

The authors declare that they have no known competing financial interests or personal relationships that could have appeared to influence the work reported in this paper.

DATA AVAILABILITY

Data will be made available on request

ACKNOWLEDGEMENTS

This research is supported by High-performance Computing Platform of Southwest Minzu University, and Southwest Minzu University Research Startup Funds (YCZD2024022).

REFERENCES

[1] H. Wang, G. Wang, J. Qi, H. Schandl, Y. Li, C. Feng, X. Yang, Y. Wang, X. Wang. S. Liang, Scarcity-weighted fossil fuel footprint of China at the provincial level, Appl. Energy 258 (2020) 114081.
[2] L. Suo, F. Han, X. Fan, H. Liu, K. Xu, C. Wang, “Water-in-salt” electrolytes enable green and safe Li-ion batteries for large scale electric energy storage applications, J. Mater. Chem. A 4 (2016) 6639-6644.
[3] H. Zhou, Y. Wang, H. Li, P. He, The development of a new type of rechargeable batteries based on hybrid electrolytes, ChemSusChem 3 (2010) 1009-1019.
[4] C. Du, Z. Zhao, H. Liu, F. Song, L. Chen, Y. Cheng, Z. Guo, The status of representative anode materials for lithium-ion batteries, Chem. Rec. 23 (2023) e202300004.
[5] J. Liu, Q. Duan, K. Qi, Y. Liu, J. Sun, Z. Wang, Q. Wang, Capacity fading mechanisms and state of health prediction of commercial lithium-ion battery in total lifespan, J. Energy Storage 46 (2022) 103910.
[6] D. Fan, S. Lu, C. Chen, M. Jiang, X. Li, X. Hu, Versatile two-dimensional boron monosulfide polymorphs with tunable bandgaps and superconducting properties, Appl. Phys. Lett. 117 (2020) 013103.
[7] X. Chen, Y. Zhang, The main problems and solutions in practical application of anode materials for sodium ion batteries and the latest research progress, Int. J. Energy Res. 45 (2021) 9753-9779.
[8] X. Li, L. Zhi, Graphene hybridization for energy storage applications, Chem. Soc. Rev. 47 (2018) 3189-3216.
[9] M. Weiss, R. Ruess, J. Kasnatscheew, Y. Levartovsky, N.R. Levy, P. Minnmann, L. Stolz, T. Waldmann, M. Wohlfahrt-Mehrens, D. Aurbach, M. Winter, Y. Ein-Eli.J. Janek, Fast charging of lithium-ion batteries: a review of materials aspects, Adv. Energy Mater. 11 (2021) 2101126.
[10] J. Hu, C. Ouyang, S.A. Yang. H.Y. Yang, Germagraphene as a promising anode material for lithium-ion batteries predicted from first-principles calculations, Nanoscale Horiz. 4 (2019) 457-463.
[11] A. Manthiram, A reflection on lithium-ion battery cathode chemistry, Nat. Commun. 11 (2020) 1550.
[12] L.J. Fu, K. Endo, K. Sekine, T. Takamura, Y.P. Wu. H.Q. Wu, Studies on capacity fading mechanism of graphite anode for Li-ion battery, J. Power Sources 162 (2006) 663-666.
[13] R. Zhu, C. Liu, J. Feng, Z. Guo, In situ observation of lithium dendrite of different graphite electrodes, ECS Trans. 85 (2018) 347.
[14] Y. Li, J. Song, J. Yang, A review on structure model and energy system design of lithium-ion battery in renewable energy vehicle, Renew. Sust. Energ. Rev. 37 (2014) 627-633.
[15] A. Wewer, P. Bilge, F. Dietrich, Advances of 2nd life applications for lithium ion batteries from electric vehicles based on energy demand, Sustainability 13 (2021) 5726.

[16] F.H. Gandoman, J. Jaguemont, S. Goutam, R. Gopalakrishnan, Y. Firouz, T. Kalogiannis, N. Omar, J. Van Mierlo, Concept of reliability and safety assessment of lithium-ion batteries in electric vehicles: basics, progress, and challenges, Appl. Energy 251 (2019) 113343.
[17] J. R. Dahn, T. Zheng, Y. Liu, J.S. Xue, Mechanisms for lithium insertion in carbonaceous materials, Science 270 (1995) 590-593.
[18] J. Hu, C. Ouyang, S.A. Yang, H.Y. Yang, Germagraphene as a promising anode material for lithium-ion batteries predicted from first-principles calculations, Nanoscale Horiz. 42 (2018) 457-463.
[19] Z.W. Hu, G.R. Zhang, Y. Liu, N. Liu, W. Li, J.W. Li, C.Y. Ouyang, S.A. Yang, Two-dimensional MnN utilized as high-capacity anode for Li-ion batteries, Chin. Phys. B 30 (2021) 046302.
[20] R. Rojaee, R. Shahbazian-Yassar, Two-dimensional materials to address the lithium battery challenges, ACS Nano 14 (2020) 2628-2658.
[21] C. Li, C. Zheng, F. Cao, Y. Zhang, X. Xia, The development trend of graphene derivatives, J. Electron. Mater. 51 (2022) 4107-4114.
[22] X. Peng, Q. Wei, Copple, Strain-engineered direct-indirect band gap transition and its mechanism in two-dimensional phosphorene, Phys. Rev. B 90 (2014) 085402.
[23] P. Miró, M. Ghorbani-Asl, T. Heine, Two dimensional materials beyond MoS2: noble-transition-metal dichalcogenides, Angew. Chem. Int. Ed. 53 (2014) 3015-3018.
[24] G. Barik, S. Pal, Defect induced performance enhancement of monolayer MoS2 for Li- and Na-ion batteries, J. Phys. Chem. C 123 (2019) 21852-21865.
[25] M. Salavati, T. Rabczuk, Application of highly stretchable and conductive two-dimensional 1T VS_2 and VSe2 as anode materials for Li-, Na- and Ca-ion storage, Comp. Mater. Sci. 160 (2019) 360-367.
[26] R. Meshkian, L.Å. Näslund, J. Halim, J. Lu, M.W. Barsoum, J. Rosen, Synthesis of two-dimensional molybdenum carbide, Mo2C, from the gallium based atomic laminate Mo2Ga2C, Scr. Mater. 108 (2015) 147-150.
[27] M. Naguib, J. Halim, J. Lu, K.M. Cook, L. Hultman, Y. Gogotsi. M.W. Barsoum, New two-dimensional niobium and vanadium carbides as promising materials for Li-ion batteries, J. Am. Chem. Soc. 135 (2013) 15966-15969.
[28] M. Naguib, O. Mashtalir, J. Carle, V. Presser, J. Lu, L. Hultman, Y. Gogotsi, M.W. Barsoum, Two-dimensional transition metal carbides, ACS Nano 6 (2012) 1322-1331.
[29] M. Manadé, F. Viñes. F. Illas, Transition metal adatoms on graphene: a systematic density functional study, Carbon 95 (2015) 525-534.
[30] H. Tao, Q. Fan, T. Ma, S. Liu, H. Gysling, J. Texter, F. Guo, Z. Sun, Two-dimensional materials for energy conversion and storage, Prog. Mater. Sci. 111 (2020) 100637.
[31] J. Ben, X. Liu, C. Wang, Y. Zhang, Z. Shi, Y. Jia, S. Zhang, H. Zhang, W. Yu, D. Li, X. Sun, 2D III-Nitride materials: properties, growth, and applications, Adv. Mater. 33 (2021) 2006761.
[32] H. R. Jiang, Z. Lu, M.C. Wu, F. Ciucci. TS. Zhao, Borophene: a promising anode material offering high specific capacity and high rate capability for lithium-ion batteries, Nano Energy 23 (2016) 97-104.
[33] W. Li, L. Kong, C. Chen, J. Gou, S. Sheng, W. Zhang, H. Li, L. Chen, P. Cheng. K. Wu, Experimental realization of honeycomb borophene, Sci. Bull. 63 (2018) 282-286.
[34] P. Ranjan, J.M. Lee, P. Kumar, A. Vinu, Borophene: new sensation in flatland, Adv. Mater. 32 (2020) 2000531.
[35] I. Božović, Doubling down on borophene electronics, Nat. Mater. 21 (2022) 11-12.
[36] X. Lu, M. Yu, G. Wang, T. Zhai, S. Xie, Y. Ling, Y. Tong, Y. Li, H-TiO2@MnO2//H-TiO2@C core–shell nanowires for high performance and flexible asymmetric supercapacitors, Adv. Mater. 25 (2013) 267-272.
[37] D. Geng, K. Yu, S. Yue, J. Cao, W. Li, D. Ma, B. Feng, Experimental evidence of monolayer AlB_2 with symmetry-protected Dirac cones, Phys. Rev. B 101 (2020) 161407.
[38] M. Humood, J.L. Meyer, S.V. Verkhoturov, T. Ozkan, M. Eller, E. A. Schweikert, J. Economy, A.A. Polycarpou, 2D AlB_2 flakes for epitaxial thin film growth, J. Mater. Res. 33 (2018) 2318-2326.
[39] E. Abedi, S.J. Taghizadeh Sisakht, N. Hashemifar, I. Ghafari Cherati, F.M. Abdolhosseini Sarsari, Peeters, Prediction of novel two-dimensional dirac nodal line semimetals in Al2B2 and AlB_4 monolayers, Nanoscale 14 (2022) 11270-11283.
[40] S. Ma, H. Zhang, Z. Cheng, X. Xie, X. Zhang, G. Liu. G. Chen, Two dimensional AlB_4 as high-performance anode material for Li/Na-ion batteries, Applied Surface Science 648 (2024) 159024.
[41] S. Ma, H. Zhang, N. Gao, X. Xie, Y. Fang, G. Chen, The superconducting dirac AlB_6 monolayer as an excellent anode material for Li/Na ion batteries, Mater. Today Commun. 39 (2024) 109325.

[42] G. Kresse, J. Furthmüller, Efficient iterative schemes for ab initio total-energy calculations using a plane-wave basis set, Physical Review B 54 (1996) 11169-11186.
[43] J. Hafner, Ab-initio simulations of materials using VASP: density-functional theory and beyond, J. Comput. Chem. 29 (2008) 2044-2078.
[44] S. Grimme, Semiempirical GGA-type density functional constructed with a long-range dispersion correction, J. Comput. Chem. 27 (2006) 1787-1799.
[45] J. P. Perdew, K. Burke, M. Ernzerhof, Generalized gradient approximation made simple, Phys. Rev. Lett. 77 (1996) 3865-3868.
[46] K. Choudhary, F. Tavazza, Convergence and machine learning predictions of monkhorst-pack k-points and plane-wave cut-off in high-throughput DFT calculations, Comp. Mater. Sci. 161 (2019) 300-308.
[47] H. J. Monkhorst, J. D. Pack, special points for brillouin-zone integrations, Phys. Rev. B 13 (1976) 5188-5192.
[48] A. Yadav, C. M. Acosta, G. M. Dalpian, O. I. Malyi, First-principles investigations of 2D materials: challenges and best practices, Matter 6 (2023) 2711-2734.
[49] S. Grimme, J. Antony, S. Ehrlich, H. Krieg, A consistent and accurate ab initio parametrization of density functional dispersion correction (DFT-D) for the 94 elements H-Pu, J. Chem. Phys. 132 (2010) 154104.
[50] B. Kirchner, P. di Dio. J. Hutter, Real-world predictions from Ab initio molecular dynamics simulations, Top. Curr. Chem. 307 (2011) 109-153.
[51] V. Palomares, N. Nieto, T. Rojo, Negative electrode materials for high-energy density Li- and Na-ion batteries, Curr. Opin. Electrochem. 31 (2022) 100840.
[52] T. Kim, W. Song, DY. Son, L.K. Ono,Y. Qi, Lithium-ion batteries: outlook on present, future, and hybridized technologies, J. Mater. Chem. A 7 (2019) 2942-2964.
[53] W. Li, Y. Yang, G. Zhang. Y.W. Zhang, Ultrafast and directional diffusion of lithium in phosphorene for high-performance lithium-ion battery, Nano Lett. 15 (2015) 1691-1697.
[54] L. Benitez, J. Seminario, Ion diffusivity through the solid electrolyte interphase in lithium-ion batteries, J. Electrochem. Soc. 164 (2017) 3159-3170.
[55] K. Persson, V.A. Sethuraman, L.J. Hardwick, Y. Hinuma, Y.S. Meng, A. van der Ven, V. Srinivasan, R. Kostecki, G. Ceder, Lithium diffusion in graphitic carbon, J. Phys. Chem. Lett. 1 (2010) 1176-1180.
[56] J. Rehman, R. Ali, N. Ahmad, X. Lv, C. Guo, Theoretical investigation of strain-engineered WS_{e2} monolayers as anode material for Li-ion batteries, J. Alloys Compd. 804 (2019) 370-375.
[57] E. Pollak, B. Geng, K.J. Jeon, I.T. Lucas, T.J. Richardson, F. Wang, R. Kostecki, The interaction of Li+ with single-layer and few-layer graphene, Nano Lett. 10 (2010) 3386-3388.
[58] J. Setiadi, M. D. Arnold, M.J. Ford, Li-ion adsorption and diffusion on two-dimensional silicon with defects: a first principles study, ACS Appl. Mater. Interfaces 5 (2013) 10690-10695.
[59] S. Thomas, A.K. Madam. M.A. Zaeem, Stone–wales defect induced performance improvement of BC_3 monolayer for high capacity lithium-ion rechargeable battery anode applications, J. Phys. Chem. C 124 (2020) 5910-5919.
[60] F. Li, Y. Qu, M. Zhao, Germanium sulfide nanosheet: a universal anode material for alkali metal ion batteries, J. Mater. Chem. A 4 (2016) 8905-8912.
[61] S. Zhao, W. Kang, J. Xue, The potential application of phosphorene as an anode material in Li-ion batteries, J. Mater. Chem. A 2 (2014) 19046-19052.
[62] V. Shukla, R. B. Araujo, N. K. Jena, R. Ahuja, The curious case of two dimensional Si_2BN: a high-capacity battery anode material, Nano Energy 41 (2017) 251-260.
[63] Y. Dong, W. Wei, X. Lv, B. Huang, Y. Dai, Semimetallic Si_3C as a high capacity anode material for advanced lithium ion batteries, Appl. Surf. Sci. 479 (2019) 519-524.
[64] Y. Wang, H. Fang, L. Zhou, T. Wada, Revisiting the state-of-charge estimation for lithium-ion batteries: a methodical investigation of the extended kalman filter approach, IEEE Control Syst. 37 (2017) 73-96.
[65] X. J. Ye, J. Xu, Y.D. Guo, C. S. Liu, Metallic two-dimensional BP2: a high-performance electrode material for Li- and Na-ion batteries, Phys. Chem. Chem. Phys. 23 (2021) 4386-4393.
[66] G. Yuan, T. Bo, X. Qi, P.F. Liu, Z. Huang, B. T. Wang, Monolayer Zr2B2: A promising two-dimensional anode material for Li-ion batteries, Appl. Surf. Sci. 480 (2019) 448-453.
[67] J. Hu, B. Xu, C. Ouyang, Y. Zhang, S A. Yang, Investigations on Nb2C monolayer as promising anode material for Li or non-Li ion batteries from first-principles calculations, RSC Adv. 6 (2016) 27467-27474.

[68] Y. Jing, Z. Zhou, C. Cabrera, Z. Chen, Metallic VS_2 monolayer: a promising 2D anode material for lithium ion batteries, J. Phys. Chem. C 117 (2013) 25409–25413.
[69] D. Er, J. Li, M. Naguib, Y. Gogotsi, V.B. Shenoy, Ti_3C_2 MXene as a high capacity electrode material for metal (Li, Na, K, Ca) ion batteries, ACS Appl. Mater. Interfaces 6 (2014) 11173-11179.
[70] D. Wang, Y. Gao, Y. Liu, D. Jin, Y. Gogotsi, X. Meng, F. Du, G. Chen, Y. Wei, First-principles calculations of Ti2N and Ti2NT2 (T = O, F, OH) monolayers as potential anode materials for lithium-ion batteries and beyond, J. Phys. Chem. C 121 (2017) 13025-13034.
[71] Y. M. Li, W. G. Chen, Y. L. Guo, Z. Y. Jiao, Theoretical investigations of TiNbC MXenes as anode materials for Li-ion batteries, J. Alloys Compd. 778 (2019) 53-60.
[72] Y. Zhou, C. Geng, A MoO2 sheet as a promising electrode material: ultrafast Li-diffusion and astonishing Li-storage capacity, Nanotechnology 28 (2017) 105402.
[73] H. Liu, Y. Cai, Z. Guo, J. Zhou, Two-dimensional V2N mxene monolayer as a high-capacity anode material for lithium-ion batteries and beyond: first-principles calculations, ACS Omega 7 (2022) 17756-17764.
[74] A. Sengupta, First principles study of Li adsorption properties of a borophene based hybrid 2D material B5Se, Appl. Surf. Sci. Adv. 8 (2022) 100218.
[75] B. Pan, D. Dong, J. Wang, J. Nie, S. Liu, Y. Cao, Y. Jiang, Aging mechanism diagnosis of lithium ion battery by open circuit voltage analysis, Electrochim. Acta 362 (2020) 137101.
[76] J. Song, M. Jiang, C. Wan, H. Li, Q. Zhang, Y. Chen, X. Wu, X. Yin, J. Liu, Defective graphene/SiGe heterostructures as anodes of Li-ion batteries: a first-principles calculation study, Phys. Chem. Chem. Phys. 25 (2023) 617-624.
[77] Z. W. Seh, Y. Sun, Q. Zhang, Y. Cui, Designing high-energy lithium–sulfur batteries, Chem. Soc. Rev. 45 (2016) 5605-5634.
[78] Q. Sun, Y. Dai, Y. Ma, T. Jing, W. Wei, B. Huang, Ab initio prediction and characterization of Mo2C monolayer as anodes for lithium-ion and sodium-ion batteries, J. Phys. Chem. Lett. 7 (2016) 937-943.
[79] T. Bo, P.F. Liu, J. Zhang, F. Wang, B.T. Wang, Tetragonal and trigonal Mo2B2 monolayers: two new low-dimensional materials for Li-ion and Na-ion batteries, Phys. Chem. Chem. Phys. 21 (2019) 5178-5188.